HDL-TM-91-16

October 1991

Theoretical Crystal-Field Calculations for Rare-Earth Ions in III-V Semiconductor Compounds

by Sally B. Stevens
Clyde A. Morrison

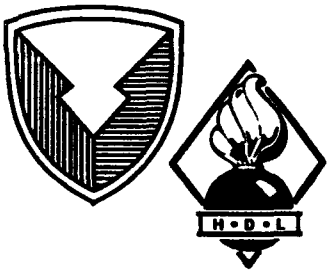

U.S. Army Laboratory Command
Harry Diamond Laboratories
Adelphi, MD 20783-1197

The findings in this report are not to be construed as an official Department of the Army position unless so designated by other authorized documents.

Citation of manufacturers' or trade names does not constitute an official endorsement or approval of the use thereof.

Destroy this report when it is no longer needed. Do not return it to the originator.

REPORT DOCUMENTATION PAGE

Form Approved
OMB No. 0704-0188

1. AGENCY USE ONLY *(Leave blank)*	2. REPORT DATE	3. REPORT TYPE AND DATES COVERED
	October 1991	Summary, from Jan 91 to Jul 91

4. TITLE AND SUBTITLE
Theoretical Crystal-Field Calculations for Rare-Earth Ions in III-V Semiconductor Compounds

5. FUNDING NUMBERS
PE: P6

6. AUTHOR(S)
Sally B. Stevens and Clyde A. Morrison

7. PERFORMING ORGANIZATION NAME(S) AND ADDRESS(ES)
Harry Diamond Laboratories
2800 Powder Mill Road
Adelphi, MD 20783-1197

8. PERFORMING ORGANIZATION REPORT NUMBER
HDL-TM-91-16

9. SPONSORING/MONITORING AGENCY NAME(S) AND ADDRESS(ES)
U.S. Army Laboratory Command
2800 Powder Mill Road
Adelphi, MD 20783-1145

10. SPONSORING/MONITORING AGENCY REPORT NUMBER

11. SUPPLEMENTARY NOTES
AMS code: P612120H25
HDL PR: 1R8A51

12a. DISTRIBUTION/AVAILABILITY STATEMENT
Approved for public release; distribution unlimited.

12b. DISTRIBUTION CODE

13. ABSTRACT *(Maximum 200 words)*

This report presents preliminary crystal-field calculations showing the splitting of the Stark levels of three rare-earth-doped III-V semiconductor compounds: Yb^{3+}:InP, Er^{3+}:GaAs, and Nd^{3+}:GaP. The crystal-field parameters were obtained from a lattice-sum calculation including monopole, self-induced dipole, and self-induced quadrupole contributions. The effects of varying the effective ionic charges and the ionic polarizabilities are explored. For each of the systems considered, these parameters were adjusted to match available experimental data on the ordering of the levels according to irreducible representation, the magnitude of crystal-field splitting, and intensities. A consistent set of parameters was found that gave reasonable results for all the systems considered. Refinements in the crystal-field model may be necessary when more experimental data become available.

14. SUBJECT TERMS	15. NUMBER OF PAGES
Rare earth, semiconductor, crystal-field theory	28
	16. PRICE CODE

17. SECURITY CLASSIFICATION OF REPORT	18. SECURITY CLASSIFICATION OF THIS PAGE	17. SECURITY CLASSIFICATION OF ABSTRACT	20. LIMITATION OF ABSTRACT
Unclassified	Unclassified	Unclassified	UL

NSN 7540-01-280-5500

Standard Form 298 (Rev 2-89)
Prescribed by ANSI Std Z39 18
298 102

Contents

Figures

Tables

Tables (cont'd)

1. Introduction

The incorporation of rare-earth ions into III-V semiconductor compounds has recently generated a great deal of interest, motivated primarily by potential applications in optoelectronic devices. Many groups have reported photoluminescence and photoluminescence excitation measurements of rare-earth ions in these systems. The systems for which the most published data are available are Yb^{3+}:InP, Er^{3+}:GaAs, and Nd^{3+}:GaP (we provide bibliographies for each of these). In addition, two review articles have been written [1,2], and some work has been done on theory [3].

The symmetry of the site occupied by the rare-earth ion depends on the growth conditions. For the samples listed above, the sample preparation has been optimized to minimize the number of lines seen in the spectrum. It is assumed that under favorable growth conditions, the rare-earth ion substitutes for a cation. For unfavorable growth conditions, it has been speculated that the rare-earth ion occupies an interstitial site or defect site instead of substituting for a cation. The location of the rare-earth ion in a III-V lattice is discussed by Kozanecki et al [4,5]. Because Yb is the smallest rare-earth ion and In is larger than Ga or Al, Yb^{3+}:InP grows relatively easily with Yb substituting for indium in the InP lattice. For the other systems considered, the optimum conditions for sample growth are still under investigation, but many of the spectral features can be explained assuming cubic symmetry.

The starting point for each sample considered is a simple point-charge model with full valence charges (±3) for the constituent ions. Variations of the simple point-charge model are considered that give improved agreement to the experimental data. The irreducible representations are obtained from group theory, assuming T_d symmetry of the rare-earth site. Varying the effective ionic charge changes the relative splitting of the levels but not the ordering of the irreducible representations. Introducing self-induced contributions to the simple point-charge model allows the relative ordering of the irreducible representations to be changed, as well as the magnitude of the level splittings.

Physically reasonable values for the material parameters (the effective charge and the dipole and quadrupole polarizabilities) are discussed in section 2. For each of the three systems considered, the parameters $Q = 3$, $\alpha_D = 2$ Å^3, and $\alpha_Q = 4$ Å^5 provide a good starting point for interpreting experimental data, and the results of the calculations using these parameters are presented in sections 3 to 5. For Er^{3+}:GaAs, sufficient experimental data are available so that we can deviate from this parameter combination to improve agreement with the data. For all the systems considered, the identification of the levels is uncertain because of the presence of extra lines, and further optimization of

the model may be more profitable after more experimental work is done. As a complement to the energy level calculation, the relative intensities of transitions measured in fluorescence are also calculated directly from the theoretical model. The intensity calculations were done at 6 K to correspond to experimental fluorescence measurements. At this temperature, essentially all transitions originate at the lowest level of the upper multiplet. These calculations are compared directly with the photoluminescence spectra and provide a further check on the model.

2. Material Properties

2.1 Crystallographic Data

The III-V semiconductor compounds considered in this report crystallize in the zinc-blende structure, which belongs to space group $F\bar{4}3m$, 216 in the *International tables for x-ray crystallography* [6]. The lattice is described in Wyckoff [7] with two sites, the cation and anion sites, each having T_d symmetry. The crystallographic information is summarized in table 1. The lattice parameters for these compounds are also given by Wyckoff as 5.6537 Å for GaAs, 5.8687 Å for InP, and 5.4505 Å for GaP.

Table 1. Fractional positions of atoms in unit cell

Site	Symmetry	x	y	z	Charge	Dipole polarizability	Quadrupole polarizability
Cation site (Ga, In)	T_d	0	0	0	$+Q$	$\alpha_D(+)$	$\alpha_Q(+)$
Anion site (As, P)	T_d	0.25	0.25	0.25	$-Q$	$\alpha_D(-)$	$\alpha_Q(-)$
Interstitial sites	T_d	0.50	0.50	0.50	—	—	—
	T_d	0.75	0.75	0.75	—	—	—

2.2 Effective Charges

To maintain charge neutrality, the effective cation charge, Q, is balanced by an anion charge, $-Q$, giving only one free parameter for the effective charge. Various models have been developed to describe the effective charge in III-V compounds [8,9]. In the simplest approximation, the static effective charge can be written $Q^* = -\Delta Q + 4p$, where $0 \leq p \leq 1$, and $\Delta Q = 1$ for III-V compounds. For $p = 1$, the effective cation charge is the full valence charge of +3 (in units of the electronic charge). The models predict an effective cation charge somewhat smaller than the full valence charge $Q = 3$, but not a great deal smaller. The effective charges calculated from a band-structure model [9] range from 2.0 to 2.5.

In T_d symmetry, there are four nonzero even-k crystal-field components, but only B_{40} and B_{60} are independent; $B_{44} = (5/14)^{1/2} B_{40}$ and $B_{64} = -(7/2)^{1/2} B_{60}$. If dipole and quadrupole polarizabilities as well as the effective charge

are allowed to vary, there are more free parameters in the model than independent crystal-field components. For this reason, the effective charge was fixed at $Q = 3$. A point-charge model with effective charge $Q = 3$ and no self-induced terms is subsequently referred to as a simple point-charge model.

2.3 Polarizabilities

In sites with cubic symmetry, there are no point-dipole or point-quadrupole contributions because of the high symmetry of the lattice [10]. However, the cubic symmetry does not prevent self-induced effects. We have calculated these effects following Morrison et al [11]. Table 2 lists the contributions to the crystal-field components, A_{kq}, for each ion from the monopole, self-induced dipole, and self-induced quadrupole terms, with unit charge and unit polarizabilities for all ionic species. The contributions are multiplied by the parameters Q, α_D, and α_Q for each species and added to compute the total crystal field. Very nearly all the self-induced contributions come from the anion, and to a good approximation, the cation contributions to the self-induced fields can be neglected, even though the calculated polarizabilities for the cations are larger than for the anions. This gives two parameters for the anion polarizabilities, α_D and α_Q, in addition to the effective charge, Q, for each compound.

Dipole polarizabilities have been computed by Pandey et al [12] for several III-V compounds and are given in table 3. They used the Clausius-Mossotti relation, which is of questionable applicability to III-V compounds. It should be possible to repeat these calculations with an effective electric field appropriate to semiconductors [13]. Theoretical dipole ionic polarizabilities for positive ions can be calculated from Hartree-Fock theory and have been tabulated by Fraga, Karwowski, and Saxena [14]. However, since the positive ionic contributions to the self-induced fields are not significant, we have not made use of these values. Dipole and quadrupole polarizabilities for several ions are given by Schmidt et al [15]. Although neither P^{3-} nor As^{3-} is included in this study, N^{3-} is, and one may assume that the values for the other column-V elements are comparable. For N^{3-}, $\alpha_D = 2.65$ Å^3 and $\alpha_Q = 12.12$ Å^5. These values are large, and in light of previous experience [11], we reduced these values in simulating the experimental data. The splittings produced by these parameters for each of the compounds considered are described in the following sections.

If the formulas in the paper by Morrison et al [11] are used, the higher order multipoles could also be included, but there are no reliable estimates of polarizabilities for higher order multipoles. The quality of the fluorescence data at this time does not warrant the determination of polarizabilities from spectral analysis, so estimates of the magnitude of the multipolar polarizabili-

ties need to come from other measurements. It is expected that the contributions from higher order multipoles will become progressively weaker, although we have no data to substantiate this claim.

Table 2. Multipole contributions to crystal-field components, A_{kq}
These contributions are multiplied by the parameters Q, α_D, and α_Q, respectively, for each ionic species and added to compute the total crystal field.

a. In site in InP

A_{kq}	Monopole		Self-induced dipole		Self-induced quadrupole	
($cm^{-1}/Å^k$)	In	P	In	P	In	P
Im A_{32}	0	−5492	0	−848.9	0	−331.3
A_{40}	125.9	1659	8.65	428.4	1.58	199.7
A_{44}	75.3	992	5.17	256.0	0.94	119.3
A_{60}	12.9	−151	1.58	−78.3	0.37	−48.5
A_{64}	−24.1	283	−2.95	146.5	−0.69	90.7
Im A_{72}	0	86.2	0	57.6	0	40.1
Im A_{76}	0	79.3	0	53.0	0	36.9

b. Ga site in GaAs

A_{kq}	Monopole		Self-induced dipole		Self-induced quadrupole	
($cm^{-1}/Å^k$)	Ga	As	Ga	As	Ga	As
Im A_{32}	0	−6376.4	0	−1102.4	0	−463.5
A_{40}	151.8	1999.7	11.7	577.4	2.29	290.0
A_{44}	90.7	1195.0	6.97	345.1	1.37	173.3
A_{60}	16.8	−196.2	2.29	−113.7	0.58	−75.9
A_{64}	−31.3	367.0	−4.28	212.7	−1.08	141.9
Im A_{72}	0	116.2	0	86.9	0	65.1
Im A_{76}	0	106.9	0	79.9	0	59.9

c. Ga site in GaP

A_{kq}	Monopole		Self-induced dipole		Self-induced quadrupole	
($cm^{-1}/Å^k$)	Ga	P	Ga	P	Ga	P
Im A_{32}	0	−7381.8	0	−1424.3	0	−644.4
A_{40}	181.9	2400.9	15.63	773.9	3.30	418.2
A_{44}	108.7	1434.8	9.34	462.5	1.97	249.9
A_{60}	21.6	−253.5	3.30	−163.9	0.89	−117.7
A_{64}	−40.5	474.2	−6.18	306.8	−1.67	220.2
Im A_{72}	0	155.7	0	129.9	0	104.8
Im A_{76}	0	143.2	0	119.5	0	96.4

Table 3. Dipole ionic polarizabilities deduced from experimental measurements of dielectric constant (Pandey et al [12])

Ion	α_D (Å^3)
Ga	4.435
In	6.489
P	2.659
As	3.786

2.4 Index of Refraction

The index of refraction is not included in the lattice model and is not necessary for calculating energy levels. It is used in the branching ratio calculations to evaluate the Lorentz inner-field correction:

$$X_{ij} = \frac{n_{ij}\left(n_{ij}^2 + 2\right)^2}{9} \text{ for electric dipole transitions, and}$$

$$X'_{ij} = n_{ij}^3 \text{ for magnetic dipole transitions.}$$

Empirical fits were made to the index of refraction data from the *CRC Handbook of Laser Science and Technology* [16] to the following Sellmeier dispersion relation:

$$n^2 = A + \frac{B\lambda^2}{\lambda^2 - C} .$$

For A not equal to one, the equation is only valid for restricted wavelength range, and the wavelength range of the input data is given in table 4 with the resulting parameter values.

Table 4. Best-fit Sellmeier coefficients for specified wavelength range

Compound	Sellmeier coefficients			Wavelength range (μm)
	A	B	C (μm²)	
GaAs	7.14	3.78	0.27	1.13–1.65
InP	5.74	3.75	0.299	0.925–2.0
GaP	5.29	3.79	0.142	0.8–3.8

3. Yb^{3+}:InP

The simple point-charge model predicts the irreducible representation of the ground state of Yb^{3+}:InP to be Γ_6. This determination is substantiated by electron paramagnetic resonance (EPR) measurements of an isotropic g-value for the ground state by Masterov et al [17] of $g = 3.29$. In pure cubic symmetry with no J-mixing, the g-values for the ground state doublets are $\Gamma_7 = 2.666$ and $\Gamma_6 = 3.4$. In order to reconcile the experimental and calculated g-value for a Γ_6 doublet, we can include an orbital reduction factor $k < 1$ in calculating the $J = 7/2$ Lande g-factor [18]. It is impossible to reconcile a Γ_7 ground state with the experimental measurement of the g-value. Combinations of parameters that give a Γ_7 or Γ_8 ground state have therefore been ruled out. Because of the large energy separation of the $^2F_{7/2}$ and $^2F_{5/2}$ and the small crystal-field splitting, the J-mixing by the crystal field has a negligible effect on the g-factors.

The contributions of the monopole and self-induced terms to the crystal-field parameters for Yb^{3+}:InP are given in table 5. The crystal-field parameters, B_{kq}, are related to the crystal-field components, A_{kq}, by $B_{kq} = \rho_k A_{kq}$. Values of ρ_k for Yb^{3+} ($\rho_4 = 0.3938$ and $\rho_6 = 0.912$) are given by Morrison and Leavitt [19]. All the nonzero tensor components, A_{kq} and B_{kq}, are listed in table 5 for the sake of completeness, even though they are not all independent. The theoretical energies and irreducible representations corresponding to these crystal-field parameters are given in table 6 and depicted schematically in figure 1.

The first point of comparison with the experimental data is the ordering of the irreducible representations. As mentioned above, theory and EPR measurements both give Γ_6 as the ground state. Several papers [20–23] have identified the lowest state in the upper multiplet as a Γ_8 quartet. This is stated most explicitly by Aszodi et al [22], where two different sets of crystal-field parameters are used to describe the upper and lower multiplets. Using the present approach, we cannot justify the use of the two sets of parameters from a microscopic point of view. For all parameter combinations that give a Γ_6 ground state, the lowest level in the $^2F_{5/2}$ multiplet is also a Γ_6 doublet. The present results suggest that the line chosen for Zeeman analysis was not the line corresponding to a transition from the lowest $^2F_{5/2}$ level to the ground state, as assumed by the authors.

Table 5. Crystal-field parameters for Yb^{3+}:InP with Q(In) = +3, and Q(P) = −3, and phosphorus polarizabilities α_D = 2.0 Å^3 and α_Q = 4.0 Å^5

A_{kq} (cm^{-1}/Å^k)	Monopole	Self-induced dipole	Self-induced quadrupole	Total crystal field	B_{kq} (cm^{-1})
Im A_{32}	16,476.3	−1697.8	−1325.2	13,453.3	—
A_{40}	−4,599.9	856.7	798.6	−2,944.5	−1159.5
A_{44}	−2,749.0	512.0	477.3	−1,759.7	−693.0
A_{60}	491.9	−156.6	−193.9	141.4	128.9
A_{64}	−920.3	292.9	362.8	−264.5	−241.2
Im A_{72}	−258.6	115.3	160.4	17.1	—
Im A_{76}	−237.9	106.0	147.6	15.7	—

Table 6. Energy levels for Yb^{3+}:InP computed using crystal-field parameters of table 5

$^{2S+1}L_J$ (centroid)	Level	Γ_n	Theoretical energy (cm^{-1})	Theoretical energy shifted by 10,338 cm^{-1}	Experimental energy (cm^{-1})
$^2F_{7/2}$	1	6	0.1	−10,338	—
(294.7)	2	8	348	−9,990	−9,990
	3	7	475	−9,863	−9,921
$^2F_{7/2}$	4	6	10,338	0	0
(10,553.4)	5	8	10,665	327	—

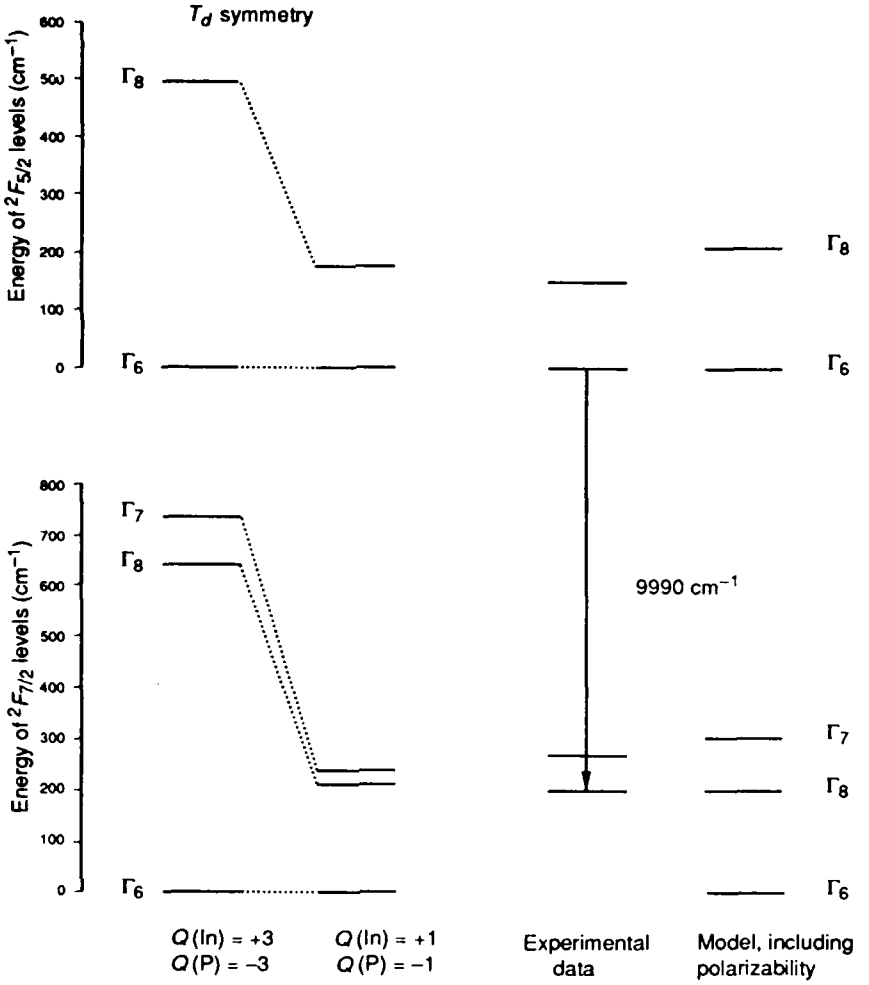

Figure 1. Energy level diagram for Yb^{3+}:InP.

The second point of comparison is the magnitude of the crystal-field splittings. The strongest lines in the spectrum are seen at 9990 and 9921 cm^{-1}, yielding a splitting between the second and third lines in the lower multiplet of 69 cm^{-1} [20–22]. A peak is seen 35 cm^{-1} below the strong peak at 9990 cm^{-1} in photoluminescence measurements [20–22] and was identified as the transition to the ground state. However, the theoretical calculation places the ground state 348 cm^{-1} below the Γ_8 level. The transition to the ground state connects two Γ_6 states, and since this transition is not allowed by electric dipole selection rules, it is expected to be weak. A line at a higher frequency was reported by Kozanecki et al [23] and shown (on a scale expanded by a factor of 15) together with the strong transitions at 9921 and 9990 cm^{-1}. Kozanecki et al did not report a numerical value for the energy, but from the plot of their data, the line is at approximately 10,135 cm^{-1}, and the line at this energy is a possible candidate for the transition connecting the two Γ_6 states. Because the transition to the ground state is expected to be very weak, it is easily confused with other extra lines in the spectra and may be difficult to identify experimentally.

The centroid for the $^2F_{5/2}$ multiplet is adjusted in table 6 to reproduce the splitting at 9990 cm^{-1}. This raises the center of gravity of the upper multiplet by around 100 cm^{-1} from what was reported elsewhere [20–22], bringing it into closer agreement with the center of gravity for this multiplet in other insulating crystals (see, for example, the review article in Gschneidner and Eyring [24]). Since the host material, rather than the atomic parameters, should have the largest influence on the crystal-field splittings, the higher placement of the centroid has more credibility.

Figure 2 shows branching ratios for Yb^{3+}:InP calculated using the odd-fold crystal-field components given in table 5. The strongest transition is predicted as the transition from Γ_6 ($J = 5/2$) to a Γ_8 ($J = 7/2$) at 9990 cm^{-1}. Experimentally, the line at 9990 cm^{-1} is strong, but the line at 9921 cm^{-1} is almost as strong and has structure. No detailed quantitative comparison is made with the experimental luminescence spectra at this time.

4. Er^{3+}:GaAs

The simple point-charge model predicts the irreducible representation of the ground state of Er^{3+}:GaAs to be Γ_6. However, EPR measurements of Er^{3+}:GaAs [25] indicate that the g-value of the ground state is isotropic ($g_{\|} = g_{\perp} = 5.921$) and corresponds well with the value appropriate for a Γ_7 state in T_d symmetry ($g(\Gamma_7) = 6.0$ and $g(\Gamma_6) = 6.8$ for perfect cubic symmetry). EPR measurements of Er^{3+}:InP [26] also indicate a Γ_7 ground state ($g_{\|} = 5.699 \pm 0.005$ and $g_{\perp} = 5.954 \pm 0.005$). The anisotropy was attributed to a slight axial distortion of the symmetry of the Er^{3+} site. One of the most successful aspects of this model is that when self-induced effects are included in the theory, the Γ_7 state is predicted to be the lowest state in the ground multiplet.

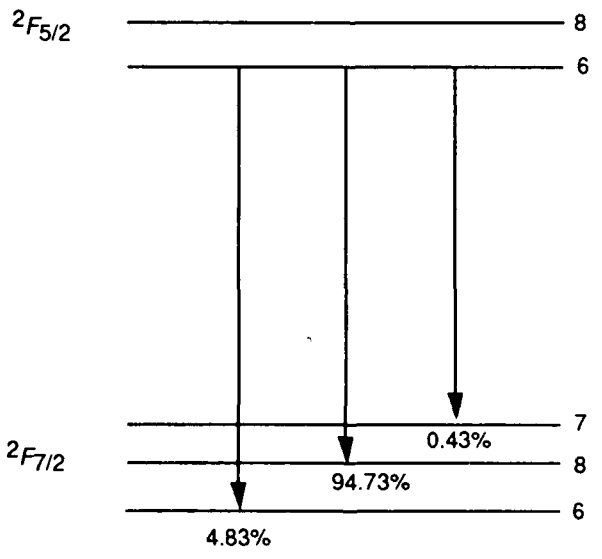

Figure 2. Branching ratios for Yb^{3+}:InP at 6 K calculated using electric and magnetic dipole transition probabilities.

The various contributions for the monopole and self-induced terms for two different parameter sets are given in table 7. The crystal-field parameters, B_{kq}, are related to the crystal-field components, A_{kq}, by $B_{kq} = \rho_k A_{kq}$. Values of ρ_k for Er^{3+} ($\rho_4 = 0.4126$ and $\rho_6 = 0.9826$) are given by Morrison and Leavitt [19]. In table 7, all the nonzero tensor components are listed for the sake of completeness, even though they are not all independent. The theoretical energies and irreducible representations of the $^4I_{15/2}$ and $^4I_{13/2}$ multiplets of Er^{3+} corresponding to the crystal-field parameters of table 7b are compared with experimental splittings in table 8, and a schematic diagram of the energy levels is shown in figure 3.

Experimental lines for the $^4I_{15/2}$ multiplet were measured by photoluminescence by Ennen et al [27]. More lines are observed in emission than expected for Er^{3+} in a cubic site. We have assumed that some of the lines are due to Er^{3+} ions in cubic sites. Extra lines may be due to ions in minority sites and phonon sidebands, especially the lines that replicate splittings observed in the upper manifold. Values for levels belonging to the $^4I_{15/2}$ multiplet not included in our calculation are 112.3, 178, 217.3, 427.9, and 449.9 cm^{-1}. A line around 30 cm^{-1} that is predicted by the model was not reported by Ennen et al [27]. Another group (Zhao et al [28]) has reported values for some of the smaller peaks with smaller splittings at 15,448, 15,482, 15,547, 15,647, and 15,685 Å. Their most intense line is the second, at 15,482 Å, which should correspond to the transition to the ground state. If splittings are measured from

Table 7. Crystal-field parameters for Er^{3+}:GaAs, for Q(Ga) = +3, and Q(As) = −3

a. Arsenic polarizabilities $\alpha_D = 2$ Å^3 and $\alpha_Q = 4$ Å^5

A_{kq} (cm^{-1}/Å^k)	Monopole	Self-induced dipole	Self-induced quadrupole	Total crystal field	B_{kq} (cm^{-1})
Im A_{32}	19,129.2	−2204.7	−1854.2	15,070.3	—
A_{40}	−5,543.7	1154.9	1159.9	−3,228.9	−1332.2
A_{44}	−3,313.0	690.2	693.2	−1,929.6	−796.2
A_{60}	638.8	−227.4	−303.5	107.9	106.0
A_{64}	−1,195.1	425.5	567.8	−201.8	−198.3
Im A_{72}	−348.6	173.8	260.6	85.8	—
Im A_{76}	−320.6	159.8	239.7	78.9	—

b. Arsenic polarizabilities $\alpha_D = 1.7$ Å^3 and $\alpha_Q = 3.4$ Å^5

A_{kq} (cm^{-1}/Å^k)	Monopole	Self-induced dipole	Self-induced quadrupole	Total crystal field	B_{kq} (cm^{-1})
Im A_{32}	19,129.2	−1874.0	−1576.1	15,679.1	—
A_{40}	−5,543.7	981.7	986.0	−3,576.1	−1475.5
A_{44}	−3,313.0	586.7	589.2	−2,137.1	−881.8
A_{60}	638.8	−193.3	−258.0	187.5	184.2
A_{64}	−1,195.1	361.6	482.6	−350.8	−344.7
Im A_{72}	−348.6	147.7	221.5	20.6	—
Im A_{76}	−320.6	135.9	203.7	19.0	—

Table 8. Energy levels for Er^{3+}:GaAs computed using crystal-field parameters of table 7b

$2S+1L_J$ (centroid)	Level	Γ_n	Theoretical energy (cm^{-1})	Experimental energy (cm^{-1}) strongest lines
$^4I_{15/2}$ (162.8)	1	7	0.0	0
	2	8	29.0	—
	3	6	71	69.4
	4	8	265	268.5
	5	8	301	—
$^4I_{13/2}$ (6610.8)	6	8	6501	6500.7
	7	6	6528	6569.0
	8	6	6639	6627.3
	9	8	6679	6680.5
	10	7	6708	6715.0

Figure 3. Energy level diagram for Er^{3+}:GaAs.

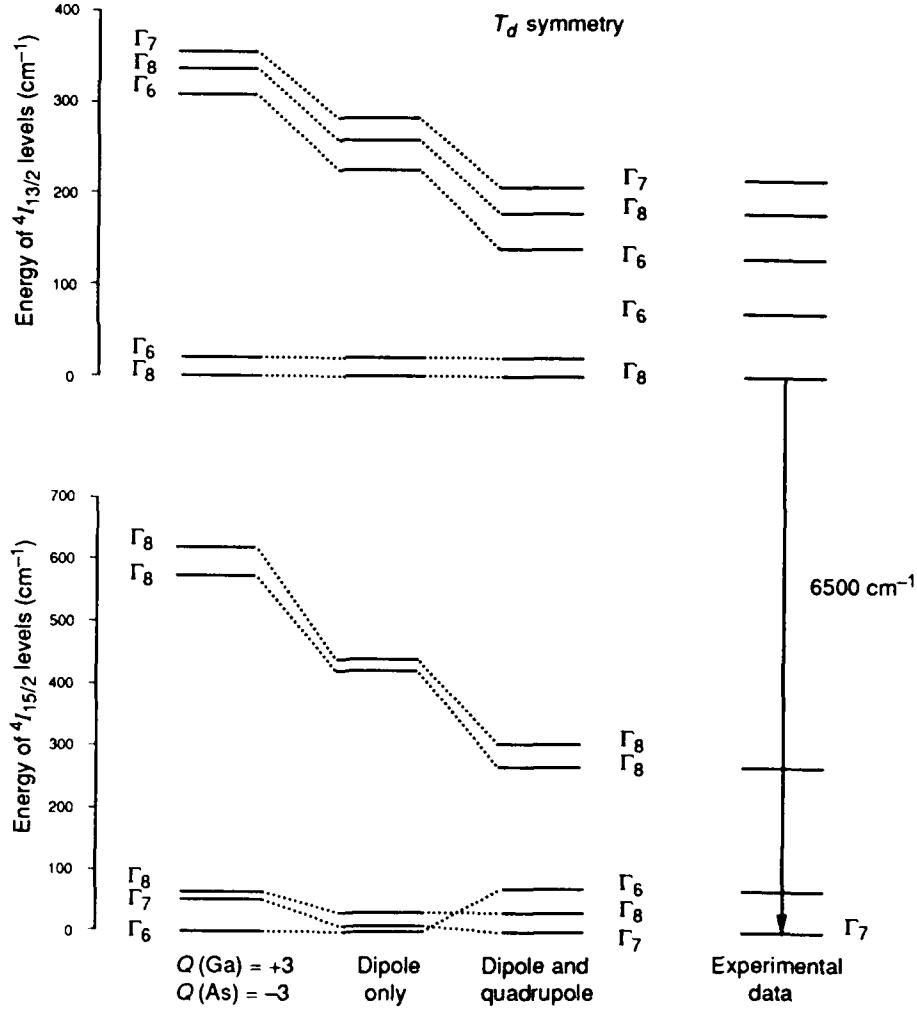

this line, the next three lines are at 26, 68, and 83 cm^{-1}. These peaks are visible in the spectrum of Ennen et al, but were not labelled as erbium peaks. If their three lowest levels (0, 69, and 112 cm^{-1}) are fit assuming cubic symmetry, the parameter values again correspond to ionic charges larger than ±3. In general, it is more difficult to fit data measured in emission than in absorption, and it is hard to conclude anything from the emission spectrum alone.

Experimental lines for the $^4I_{13/2}$ multiplet were measured by photoluminescence excitation spectroscopy by Ennen et al [27]. The weak pair of levels at 6840.4 and 6854.3 cm^{-1} was not included in table 8. Splitting the upper manifold this strongly, assuming cubic symmetry, would require a point-charge model with ionic charges larger than ±3. The other levels in the upper multiplet correlate reasonably well with the levels predicted by the model.

Branching ratios for Er^{3+}:GaAs are given in figure 4. In agreement with experiment, the model predicts the strongest intensity at low temperatures in the transition from the lowest state of the upper multiplet to the ground state.

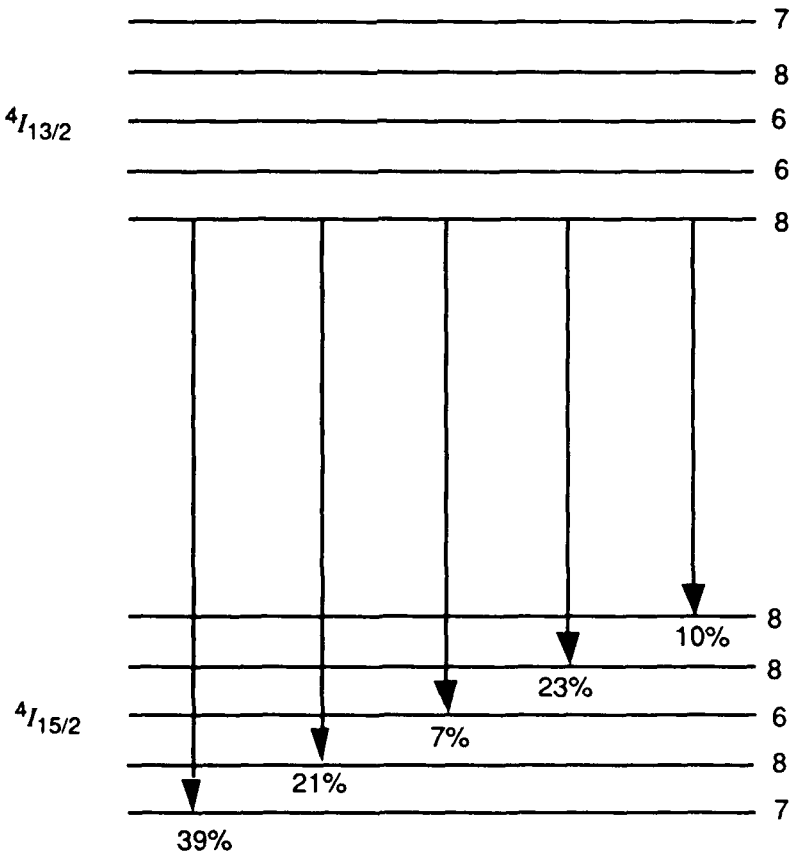

Figure 4. Branching ratios for Er^{3+}:GaAs at 6 K calculated using electric and magnetic dipole transition probabilities.

5. Nd^{3+}:GaP

Of the three systems described in this report, the least amount of experimental work has been published for Nd^{3+}:GaP. In computing the theoretical levels, the same parameter values giving reasonable results for the other two ions were used in the lattice sum for GaP: $Q = 3.0$, $\alpha_D = 2.0$ Å^3, and $\alpha_Q = 4.0$ Å^5; the results are presented in table 9. The crystal-field calculation based on these parameters is given in table 10. No EPR data were found for this system. Photoluminescence data have been reported by Müller et al [29] and Donegan [30]. Müller et al have reported that two sets of lines are evident in the spectrum, but one set decreases in intensity upon annealing. The values of the more prominent set are given in table 10 (labelled as levels from the *A* complex), and the strongest lines from this set are compared with the theory.

Multiplet branching ratios for Nd^{3+}:GaP were computed for electric dipole transitions only, and the results are shown in figure 5. These results are remarkably similar to the corresponding results for the cubic material LaOF [31]. No quantitative measurements of integrated intensities are available, but one can get a qualitative estimate of the branching ratios from the photoluminescence spectra of Müller et al. The fluorescence to the $^4I_{9/2}$ multiplet is stronger than the fluorescence to the $^4I_{11/2}$ multiplet, in agreement with the calculations. Until the origin of the extra lines is better understood, it is hard to draw any strong conclusions, but the experimental results so far are consistent with a model assuming cubic symmetry.

Table 9. Crystal-field parameters for Nd^{3+}:GaP with Q(Ga) = +3 and Q(P) = −3, and phosphorus polarizabilities α_D = 2 Å^3 and α_Q = 4 Å^5

A_{kq} (cm^{-1}/Å^k)	Monopole	Self-induced dipole	Self-induced quadrupole	Total crystal field	B_{kq} (cm^{-1})
Im A_{32}	22,145.4	−2848.7	−2577.6	16,719.1	—
A_{40}	−6,657.0	1547.8	1672.6	−3,436.6	−1985.0
A_{44}	−3,978.3	925.0	999.6	−2,053.8	−1186.3
A_{60}	825.3	−327.9	−470.9	26.5	42.1
A_{64}	−1,544.1	613.5	881.0	−49.6	−78.8
Im A_{72}	−467.2	259.9	419.4	212.1	—
Im A_{76}	−429.7	239.1	385.7	195.1	—

Table 10. Energy levels for Nd^{3+}:GaP computed using crystal-field parameters from table 9

$^{2S+1}L_J$ (centroids)	Level	Γ_n	Theoretical energy (cm^{-1})	Experimental energy *A* complex (cm^{-1})	Experimental energy (cm^{-1})
$^4I_{9/2}$	1	8	0.1	0	0
(160.3)	2	8	198.1	174, 204	174
	3	7	335.3	372, 409	372
$^4I_{11/2}$	4	7	1894	1894	1894
(2022.3)	5	8	1941.5	2058, 2069	2069
	6	6	2052.8	2144	—
	7	8	2128.2	2211, 2277	—

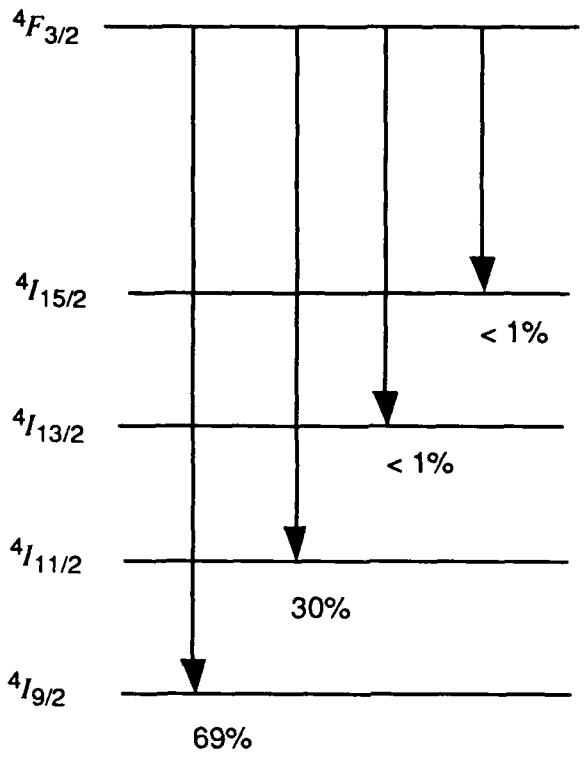

Figure 5. Multiplet branching ratios for Nd^{3+}:GaP calculated using electric dipole transition probabilities only.

6. Conclusions

The salient experimental features that need to be explained by any crystal-field model are (1) the ordering of levels according to symmetry labels, particularly correct identification of the ground state, (2) the magnitude of the crystal-field splittings, and (3) the intensities of transitions between $4f$ states.

The magnitude of the crystal-field splittings in all rare-earth ions in III-V semiconductor compounds examined so far is smaller than that produced by a point-charge model with the full valence charges. The reduced splitting can be achieved by reducing the effective ionic charges of ions in the lattice or by including self-induced contributions to the total crystal field. We have shown that the second method can better explain the experimental data and gives a more complete model of the semiconductor compounds. The rare-earth impurity ions can be used in this way as a probe to study the host in which they are embedded.

Our primary objective has been to find physically reasonable values of the parameters that accurately predict the ordering of the Stark levels. We have found that $Q = 3$, $\alpha_D = 2$ Å^3, and $\alpha_Q = 4$ Å^5 give reasonable results for all compounds considered here, and the crystal-field splittings calculated from this set of starting parameters give a good starting place for analyzing experimental data. This has worked particularly well for Er^{3+}:GaAs, where

this parameter set predicts a Γ_7 ground state in agreement with experimental EPR measurements. A point-charge model alone does not predict the correct ground state for Er^{3+}. In order to get a Γ_7 ground state without the self-induced quadrupole contribution, one must use unreasonably large values of the dipole polarizability. With physically reasonable values of dipole and quadrupole polarizabilities, the correct ground state for Er^{3+} is obtained.

More work needs to be done on the intensities, but this cannot be done until the theoretical and experimental energies are in better agreement. Several ions have shown a hypersensitivity of the optical transitions to their crystalline environment [32,33]. The theoretical intensities are not reconciled here with experimental observations, but it is noted that the intensities calculated for electric dipole transitions are sensitive to the A_{72} and A_{76} crystal-field components as well as the A_{32} component, making a complete description of the crystal field necessary.

Acknowledgements

One of the authors (SBS) held a National Research Council–HDL Research Associateship during the course of this work. Both authors wish to thank Rich Leavitt for reading the manuscript and Rich Leavitt, John Bruno, and Tom Bahder for many helpful discussions.

References

1. H. Ennen and J. Schneider, *Luminescence of rare earth ions in III-V semiconductors,* J. Electron. Mater. A **14** (1985), 115.

2. V. F. Masterov and L. F. Zakharenkov, *Rare-earth elements in III-V semiconductors (review),* Fiz. Tekh. Poluprovodn. **24** (1990), 610 [Sov. Phys. Semicond. **24** (1990), 383].

3. S. Schmitt-Rink, C. M. Varma, and A.F.J. Levi. *Excitation mechanisms and optical properties of rare-earth ions in semiconductors,* Phys. Rev. Lett. **66** (1991), 2782.

4. A. Kozanecki and R. Grötzschel, *On the location of ytterbium in GaP and GaAs lattices,* J. Appl. Phys. **64** (1988), 3315.

5. A. Kozanecki and R. Grötzschel, *Lattice location and optical activity of Yb in III-V semiconducting compounds,* J. Appl. Phys. **68** (1990), 517.

6. *International tables for x-ray crystallography,* edited by N. Henry and K. Lonsdale, Kynoch Press, Birmingham, England (1969), Vol. I.

7. R.W.G. Wyckoff, *Crystal structures*, Vol. 1, Interscience (1965), p 108.

8. W. A. Harrison and S. Ciraci, *Bond-orbital model. II*, Phys. Rev. B **10** (1974), 1516.

9. P. Vogl, *Dynamical effective charges in semiconductors: A pseudopotential approach*, J. Phys. C **11** (1978), 251.

10. C. A. Morrison, *Angular momentum theory applied to interactions in solids*, Lecture Notes in Chemistry, Vol. 47, Springer Verlag, New York (1988), p 86.

11. C. A. Morrison, G. F. de Sá, and R. P. Leavitt, *Self-induced multipole contribution to the single-electron crystal field*, J. Chem. Phys. **76** (1982), 3899.

12. R. N. Pandey, T. P. Sharma, and B. Dayal, *Electronic polarizabilities of ions in group III-V crystals*, J. Phys. Chem. Solids, **38** (1977), 329.

13. G. A. Samara, *Temperature and pressure dependences of the dielectric constants of semiconductors*, Phys. Rev. B **27** (1983), 3494.

14. S. Fraga, K. M. Saxena, and J. Karwowski, *Physical science data*: 5. *Handbook of atomic data*, Elsevier, New York (1976).

15. P. C. Schmidt, A. Weiss, and T. P. Das, *Effect of crystal fields and self-consistency on dipole and quadrupole polarizabilities of closed-shell ions*, Phys. Rev. B **19** (1979), 5525.

16. *CRC handbook of laser science and technology*, ed. M. J. Weber, Vol III, CRC Press, Inc., Florida (1986), pp 121, 202, and 203.

17. V. F. Masterov, V. V. Romanov, and K. F. Shtel'makh, *Paramagnetic resonance and relaxation of trivalent ytterbium in indium phosphide*, Sov. Phys. Solid State **25** (1983), 824.

18. A. Abragam and B. Bleaney, *Electron paramagnetic resonance of transition ions*, Clarendon Press, Oxford (1970).

19. C. A. Morrison and R. P. Leavitt, *Crystal-field analysis of triply ionized rare-earth ions in lanthanum trifluoride*, J. Chem. Phys. **71** (1979), 2366.

20. J. Wagner, J. Windscheif, and H. Ennen, *Photoluminescence excitation spectroscopy on InP:Yb*, Phys. Rev. B **30** (1984), 6230.

21. H. Ennen, G. Pomrenke, and A. Axmann, *Luminescence of the rare-earth ion ytterbium in InP, GaP, and GaAs*, J. Appl. Phys. **57** (1985), 2182.

22. G. Aszodi, J. Weber, Ch. Uihlein, P. Pu-lin, H. Ennen, U. Kaufmann, J. Schneider, and J. Windscheif, *Zeeman analysis of the ytterbium luminescence in indium phosphide*, Phys. Rev. B **31** (1985), 7767.

23. A. Kozanecki, Z. Kalinski, J. Raczynska, and J. M. Langer, *Ytterbium as a probe of the local lattice environment in $Ga_xIn_{1-x}P$ crystals*, J. Appl. Phys. **66** (1989), 3202.

24. C. A. Morrison and R. P. Leavitt, in *Handbook of the physics and chemistry of rare earths*, edited by K. A. Gschneidner and L. Eyring, North Holland, New York (1982), Vol. 5.

25. M. Baeumler, J. Schneider, F. Köhl, and E. Tomzig, *Electron spin resonance of erbium in gallium arsenide*, J. Phys. C: Solid State Phys. **20** (1987), L963.

26. V. F. Masterov, K. F. Shtel'makh, and L. F. Zakharenkov, *Electron spin resonance of Er^{3+} in indium phosphide*, Sov. Phys. Semicond. **21** (1987), 223. [Fiz. Tekh. Poluprovodn. **21** (1987), 365.]

27. H. Ennen, J. Wagner, H. D. Müller, and R. S. Smith, *Photoluminescence excitation measurements on GaAs:Er grown by molecular-beam epitaxy*, J. Appl. Phys. **61** (1987), 4877.

28. Xinwei Zhao, Kazuhiko Hirakawa, and Toshiaki Ikoma, *Intracenter transitions in triply ionized erbium ions diffused into III-V compound semiconductors*, Appl. Phys. Lett. **54** (1989), 712.

29. H. D. Müller, H. Ennen, J. Schneider, and A. Axmann, *Photoluminescence of neodymium-implanted gallium phosphide and gallium arsenide*, J. Appl. Phys. **59** (1986), 2210.

30. J. F. Donegan, *Observation of nonradiative energy transfer in the excitation of Nd^{3+} luminescence in GaP*, Phys. Rev. B **41** (1990), 10254.

31. K. K. Deb, R. G. Buser, C. A. Morrison, and R. P. Leavitt, *Crystal fields and intensities of triply ionized rare-earth ions in cubic lanthanum oxyfluoride: An efficient $^4F_{3/2} \rightarrow {}^4I_{9/2}$ LaOF:Nd laser*, J. Opt. Soc. Am. **71** (1981), 1463.

32. B. R. Judd, *Ionic transitions hypersensitive to environment*, J. Chem. Phys. **70** (1979), 4830.

33. G. Lacueva and A. W. Overhauser, *Superallowed electric-quadrupole transitions of ions in crystals*, Phys. Rev. Lett. **63** (1989), 1716.

Bibliography of Erbium-, Ytterbium-, and Neodymium-Doped III-V Semiconductors

Er

F. Auzel and A. M. Jean-Louis, *Oscillator strengths, quantum efficiencies, and laser cross sections of Yb^{3+} and Er^{3+} in III-V compounds,* J. Appl. Phys. **66,** 3952 (1989).

M. Baeumler, J. Schneider, F. Köhl, and E. Tomzig, *Electron spin resonance of erbium in gallium arsenide,* J. Phys. C: Solid State Phys. **20,** L963 (1987).

H. Ennen, J. Wagner, H. D. Müller, and R. S. Smith, *Photoluminescence excitation measurements on GaAs:Er grown by molecular-beam epitaxy,* J. Appl. Phys. **61,** 4877 (1987).

P. Galtier, J. P. Pocholle, M. N. Charasse, B. de Cremoux, B. Groussin, T. Benyattou, G. Guillot, and J. P. Hirtz, *1.54 μm room-temperature electroluminescence of erbium-doped GaAs and GaAlAs grown by molecular beam epitaxy,* Appl. Phys. Lett. **55,** 2105 (1989).

V. F. Masterov, K. F. Shtel'makh, and L. F. Zakharenkov, *Electron spin resonance of Er^{3+} in indium phosphide,* Sov. Phys. Semicond. **21,** 223 (1987). [Fiz. Tekh. Poluprovodn. **21,** 365 (1987).]

H. Nakagome, K. Uwai, and K. Takahei, *Extremely sharp erbium-related intra-4f-shell photoluminescence of erbium-doped GaAs grown by metalorganic chemical vapor deposition,* Appl. Phys. Lett. **53,** 1726 (1988).

C. Rochaix, A. Rolland, P. N. Favennec, B. Lambert, A. Le Corre, H. L'Haridon, and M. Salvi, *Behavior of erbium implanted in InP,* J. Electron. Mater. **17,** 351 (1986).

K. Thonke, H. U. Hermann, and J. Schneider, *A Zeeman study of the 1.54 μm transition in molecular beam epitaxial GaAs:Er,* J. Phys. C: Solid State Phys. **21,** 5881 (1988).

J. P. Van der Ziel, M. G. Oberg, and R. A. Logan, *Single longitudinal mode operation of Er-doped 1.5 μm InGaAsP lasers,* Appl. Phys. Lett. **50,** 1313 (1987).

P. S. Whitney, K. Uwai, H. Nakagome, and K. Takahei, *Erbium-doped GaAs light-emitting diodes emitting erbium f-shell luminescence at 1.54 μm,* Electron. Lett. **24,** 740 (1988).

Xinwei Zhao, Kazuhiko Hirakawa, and Toshiaki Ikoma, *Intracenter transitions in triply ionized erbium ions diffused into III-V compound semiconductors,* Appl. Phys. Lett. **54,** 712 (1989).

Yb

G. Aszodi, J. Weber, Ch. Uihlein, P. Pu-lin, H. Ennen, U. Kaufmann, J. Schneider, and J. Windscheif, *Zeeman analysis of the ytterbium luminescence in indium phosphide,* Phys. Rev. B **31**, 7767 (1985).

H. Ennen, G. Pomrenke, and A. Axmann, *Luminescence of the rare-earth ion ytterbium in InP, GaP, and GaAs,* J. Appl. Phys. **57,** 2182 (1985).

V. A. Kasatkin, F. P. Kesamanly, V. G. Makarenko, V. F. Masterov, and B. E. Samorukov, *Intracenter transitions in Yb^{3+} impurities in gallium phosphide,* Fiz. Tekh. Poluprovodn. **14**, 1832 (1980).

V. A. Kasatkin, V. F. Masterov, V. V. Romanov, B. E. Samorukiv, and K. F. Shtel'makh, *State of Yb impurities in InP crystals,* Sov. Phys. Semicond. 16, **106** (1982). [Fiz. Tekh. Poluprovodn. **16**, 173 (1982).]

W. Körber and A. Hangleiter, *Excitation and decay mechanisms of the intra-4f luminescence of Yb^{3+} in epitaxial InP:Yb layers,* Appl. Phys. Lett. **52**, 114 (1988).

A. Kozanecki and R. Grötzschel, *Lattice location and optical activity of Yb in III-V semiconducting compounds*, J. Appl. Phys. **68**, 517 (1990).

A. Kozanecki, Z. Kalinski, J. Raczynska, and J. M. Langer, *Ytterbium as a probe of the local lattice environment in $Ga_xIn_{1-x}P$ crystals*, J. Appl. Phys. **66**, 3202 (1989).

B. Lambert, Y. Toudic, G. Grandpierre, A. Rupert, and A. Le Corre, *Electrical activity of Yb in InP*, Electron. Lett. **24**, 1446 (1988).

V. F. Masterov, V. V. Romanov, and K. F. Shtel'makh, *Paramagnetic resonance and relaxation of trivalent ytterbium in indium phosphide,* Sov. Phys. Solid State **25**, 824 (1983).

K. Takahei, A. Taguchi, H. Nakagome, K. Uwai, and P. S. Whitney, *Intra-4f-shell luminescence excitation and quenching mechanism of Yb in InP*, J. Appl. Phys. **66**, 4941 (1989).

J. Wagner, J. Windscheif, and H. Ennen, *Photoluminescence excitation spectroscopy on InP:Yb,* Phys. Rev. B **30,** 6230 (1984).

Nd

J. F. Donegan, *Observation of nonradiative energy transfer in the excitation of Nd^{3+} luminescence in GaP,* Phys. Rev. B **41**, 10,254 (1990).

H. D. Müller, H. Ennen, J. Schneider, and A. Axmann, *Photoluminescence of neodymium-implanted gallium phosphide and gallium arsenide,* J. Appl Phys. **59**, 2210 (1986).

Distribution

Administrator
Defense Technical Information Center
Attn DTIC-DDA (2 copies)
Cameron Station, Building 5
Alexandria, VA 22304-6145

Director
Defense Adv. Research Projects Agency
Attn J. Friebele
1400 Wilson Blvd
Arlington, VA 22209

Director
Defense Nuclear Agency
Attn Tech Library
6801 Telegraph Road
Alexandria, VA 22310-3398

Under Secretary of Defense Research & Engineering
Attn Technical Library, 3C128
Washington, DC 20301

Commander
Atmospheric Sciences Laboratory
Attn Technical Library
White Sands Missile Range, NM 88002

Office of the Deputy Chief of Staff for Research, Development, & Acquisition
Department of the Army
Attn DAMA-ARZ-B, I. R. Hershner
Washington, DC 20310

Director
Night Vision & Electro-Optics Laboratory
Attn A. Pinto (2 copies)
Attn J. Hebersat
Attn R. Buser
Attn R. Rhode
Attn W. Tressel

Director
Night Vision & Electro-Optics Laboratory (cont'd)
Attn Technical Library
FT Belvoir, VA 22060

Director
US Army Ballistics Research Laboratory
Attn SLCBR-DD-T (STINFO)
Aberdeen Prov. Ground, MD 21005-5066

Director
US Army Electronics Warfare Laboratory
Attn AMSEL-DD
Attn AMSEL-DD, J. Charlton
FT Monmouth, NJ 07703

Commander
US Army Materials & Mechanics Research Center
Attn SLCMT-TL, Tech Library
Watertown, MA 02172

Commander
US Army Missile & Munitions Ctr & School
Attn AMSMI-TB, Redstone Sci Info Center
Attn ATSK-CTD-F
Redstone Arsenal, AL 35809

Commander
US Army Research Office Durham
Attn J. Mink
Attn C. Bogosian
Attn M. Ciftan
Attn M. Stosio
Attn R. Guenther
Research Triangle Park, NC 27709

Distribution (cont'd)

Commander
US Army Test & Evaluation Command
Attn D. H. Sliney
Attn Tech Library
Aberdeen Proving Ground, MD 21005

Commander
US Army Troop Support Command
Attn STRNC-RTL, Tech Library
Natick, MA 01762

Commanding Officer
USA Foreign Science & Technology Center
Attn AIAST-BS, Basic Science Div
Federal Office Building
Charlottesville, VA 22901

Director
Naval Research Laboratory
Attn A. Rosenbaum
Attn Code 2620, Tech Library Br
Attn Code 5554, F. Bartoli
Attn Code 5554, L. Esterowitz
Attn Code 5554, R. E. Allen
Attn Code 6540, S. R. Bowman
Attn G. Quarles
Attn G. Risenblatt
Washington, DC 20375

Commander
Naval Weapons Center
Attn Code 3854, M. Hills
Attn Code 3854, M. Nadler
Attn Code 3854, R. L. Atkins
Attn Code 3854, R. Schwartz
Attn DOCE 343, Technical Information Department
China Lake, CA 93555

Air Force Office of Scientific Research
Attn Major H. V. Winsor, USAF
Bolling AFB
Washington, DC 20332

Argonne National Laboratory
Attn W. T. Carnall
9700 South Cass Avenue
Argonne, IL 60439

Director
Advisory Group on Electron Devices
Attn Sectry, Working Group D
201 Varick Street
New York, NY 10013

NASA Langley Research Center
Attn C. Bair
Attn D. Getteny
Attn E. Filer
Attn G. Armagan
Attn J. Barnes
Attn N. Buoncristiani
Attn N. P. Barnes (2 copies)
Attn P. Cross
Hampton, VA 23665

Department of Commerce
National Bureau of Standards
Attn Library
Washington, DC 20234

Seaton Hall University
Chemistry Department
Attn H. Brittain
South Orange, NJ 07099

University of Wisconsin
Chemistry Department
Attn B. Tissue
Attn J. Wright
Madison, WI 53706

Distribution (cont'd)

Massachusetts Institute of Technology
Crystal Physics Laboratory
Attn A. Linz
Attn H. P. Jenssen
Cambridge, MA 02139

Princeton University
Department of Chemistry
Attn D. S. McClure
Attn C. Weaver
Princeton, NJ 08544

University of Minnesota, Duluth
Department of Chemistry
Attn L. C. Thompson
Duluth, MN 55812

University of Connecticut
Department of Physics
Attn R. H. Bartram
Storrs, CT 06269

San Jose State University
Department of Physics
Attn J. B. Gruber
San Jose, CA 95192

University of Virginia
Dept of Chemistry
Attn F. S. Richardson (2 copies)
Attn J. Quagliano
Charlottesville, VA 22901

Arizona State University
Dept of Chemistry
Attn L. Eyring
Tempe, AZ 85281

Johns Hopkins University
Dept of Physics
Attn B. R. Judd
Baltimore, MD 21218

University of Michigan
Dept of Physics
Attn S. C. Rand
Ann Arbor, MI 48109

Kalamazoo College
Dept of Physics
Attn K. Rajnak
Kalamazoo, MI 49007

Oklahoma State University
Dept of Physics
Attn R. C. Powell
Stillwater, OK 74078

University of Illinois
Gaseous Electronics Laboratory
Attn S. B. Stevens (10 copies)
607 E. Healey St
Champaign, IL 61820

University of Illinois
Everitt Lab
Attn J. G. Eden
1406 W. Green St
Urbana, IL 61801

Ames Laboratory Dow
Iowa State University
Attn K. A. Gschneidner, Jr. (2 copies)
Ames, IA 50011

Distribution (cont'd)

Pennsylvania State University
Materials Research Laboratory
Attn W. B. White
University Park, PA 16802

Howard University
Physics Department
Attn Prof. V. Kushamaha
25 Bryant St, NW
Washington, DC 20059

Colorado State University
Physics Department
Attn S. Kern
FT Collins, CO 80523

University of South Florida
Physics Dept
Attn R. Chang
Attn Sengupta
Tampa, FL 33620

Carnegie Mellon University
Schenley Park
Attn Physics & EE, J. O. Artman
Pittsburgh, PA 15213

University of Southern California
Attn M. Birnbaum
Denney Research Bldg, University Park
Los Angeles, CA 90089

U.P.R. 210
C.N.R.S.
Attn P. Caro
Attn P. Porcher
Attn M. Faucher
1 Place A-Briand
92195 Meudon Cédex
FRANCE

University of Dayton
Department of Chemistry
Attn S. P. Sinha
300 College Park
Dayton, OH 45469-2350

Allied Signal, Inc.
Advanced Application Dept
Attn A. Budgor
31717 La Tiemda Drive
Westlake Village, CA 91362

Aerospace Corporation
Attn M. Birnbaum
Attn N. C. Chang
PO Box 92957
Los Angeles, CA 90009

Allied Signal, Inc.
Attn R. Morris
POB 1021R
Morristown, NJ 07960

IBM Research Division
Almaden Research Center
Attn R. M. Macfarlane, Mail Stop K32
802(d)
650 Harry Road
San Jose, CA 95120

Booz-Allen & Hamilton
Attn W. Drozdoski
4330 East West Highway
Bethesda, MD 20814

Brimrose Corp of America
Attn R. G. Rosemeier
7527 Belair Road
Baltimore, MD 21236

Distribution (cont'd)

Department of Mechanical, Industrial, & Aerospace Engineering
Attn S. Temkin
PO Box 909
Piscataway, NJ 08854

McDonnell Douglas Electronic Sys Co
Dept Y440, Bldg 101, Lev 2 Rm/Pt B54
Attn MS-2066267, D. M. Andrauskas
PO Box 516
ST Louis, MO 63166

Draper Lab
Attn F. Hakimi, MS 53
555 Tech Sq
Cambridge, MA 02139

Engineering Societies Library
Attn Acquisitions Dept
345 E. 47th Street
New York, NY 10017

Fibertech, Inc.
Attn H. R. Verdun (3 copies)
510-A Herdon Pkwy
Herdon, VA 22070

Hughes Aircraft Company
Attn D. Sumida
3011 Malibu Canyon Rd
Malibu, CA 90265

Lawrence Berkeley Laboratory
Attn N. Edelstein, MS70A-1150
Berkeley, CA 94720

Director
Lawrence Radiation Laboratory
Attn H. A. Koehler
Attn M. J. Weber
Attn W. Krupke
Livermore, CA 94550

LTV
Attn M. Kock (WT-50)
PO Box 650003
Dallas, TX 75265

Martin Marietta
Attn F. Crowne
Attn J. Little, 1450
Attn P. Caldwell
Attn T. Worchesky
1450 South Rolling Rd
Baltimore, MD 21227

MIT Lincoln Lab
Attn B. Aull
PO Box 73
Lexington, MA 02173

National Oceanic & Atmospheric Adm
Environmental Research Labs
Attn Library, R-51, Tech Rpts
Boulder, CO 80302

Oak Ridge National Laboratory
Attn R. G. Haire
Oak Ridge, TN 37839

Institute for Low Temp & Struc Rsch
Polish Academy of Sciences
Attn R. Troc
50-950 Wroclaw, PO Box 937
ul. Okólna 2
POLAND

Science Applications, International Corp
Attn T. Allik
1710 Goodridge Drive
McLean, VA 22102

Shwartz Electro-Optic, Inc.
Attn G. A. Rines
45 Winthrop Street
Concord, MA 01742

Distribution (cont'd)

Southwest Research Institute
Attn M. J. Sablik
PO Drawer 28510
San Antonio, TX 78228-0510

Union Carbide Corp
Attn M. R. Kokta
50 South 32nd Street
Washougal, WA 98671

Departmento Química Fundamental
Universidade Federal de Pernambuco
Attn Gilberto de Sá
Attn A. da Gama
Attn O. Matta
Cidade Universitária
Recife, PE 50 000
BRASIL

W. J. Schafer Assoc
Attn J. W. Collins
321 Billerica Rd
Chelmsford, MA 01824

US Army Laboratory Command
Attn AMSLC-DL, Dir., Corp Labs

Installation Support Activity
Attn SLCIS-CC, Legal Office

USAISC
Attn AMSLC-IM-VA, Admin Ser Br
Attn AMSLC-IM-VP, Tech Pub Br
(2 copies)

Harry Diamond Laboratories
Attn Laboratory Directors
Attn SLCHD-TL, Library (3 copies)
Attn SLCHD-TL, Library (WRF)
Attn SLCHD-NW-E, Director

Harry Diamond Laboratories (cont'd)
Attn SLCHD-NW-EH, Chief
Attn SLCHD-NW-EP, Chief
Attn SLCHD-NW-ES, Chief
Attn SLCHD-NW-P, Chief
Attn SLCHD-NW-RF, Chief
Attn SLCHD-NW-RP, Chief
Attn SLCHD-NW-RS, Chief
Attn SLCHD-NW-TN, Chief
Attn SLCHD-NW-TS, Chief
Attn SLCHD-PO, Chief
Attn SLCHD-ST-SP, Chief
Attn SLCHD-ST-SS, Chief
Attn SLCHD-CS, J. Sattler
Attn SLCHD-NW-EP, C. S. Kenyon
Attn SLCHD-NW-EP, J. R. Miletta
Attn SLCHD-NW-RP, F. B. McLean
Attn SLCHD-NW-RS, L. Libelo
Attn SLCHD-ST-AP, T. Bahder
Attn SLCHD-ST-AP, J. Bradshaw
Attn SLCHD-ST-AP, J. Bruno
Attn SLCHD-ST-AP, E. Harris
Attn SLCHD-ST-AP, R. Leavitt
Attn SLCHD-ST-AP, J. Pham
Attn SLCHD-ST-AP, G. Simonis
Attn SLCHD-ST-AP, M. Stead
Attn SLCHD-ST-AP, M. Tobin
Attn SLCHD-ST-AP, R. Tober
Attn SLCHD-ST-AP, D. Wortman
Attn SLCHD-TA-AS, G. Turner
Attn SLCHD-ST-OP, C. Garvin
Attn SLCHD-ST-OP, J. Goff
Attn SLCHD-ST-R, A. A. Bencivenga
Attn SLCHD-ST-SP, J. Nemarich
Attn SLCHD-TA-ET, B. Zabludowski
Attn SLCTO, B. Weber
Attn SLCHD-ST-AP, C. Morrison
(10 copies)